Smart Structures and Systems, *Vol. 35*, *No. 2* (*2025*) *77-87*
https://doi.org/10.12989/sss.2025.35.2.077

Automated inspection method for reused temporary equipment members using 3D shape measurement

Jonghwa Hong [a] and Sung-Han Sim*

Department of Global Smart City, *Sungkyunkwan University*, *Suwon 16419*, *Republic of Korea*

(*Received May 30*, *2024*, *Revised December 30*, *2024*, *Accepted February 24*, *2025*)

Abstract. As the members of temporary structures at construction sites are generally reused, inspection of individual temporary equipment members before use is essential to ensure safety during construction. Visual inspection, which is a common practice for assessing the quality of reused temporary equipment, is labor-intensive and depends on the skill of the inspector; thus, automated and accurate inspection methods are desired. However, little research has been devoted to the development of such methods. Because inspection criteria are mostly relevant to deformation, the shape measurement of temporary equipment members is the most fundamental consideration. This paper proposes an automated inspection method for temporary equipment based on measured 3D (three-dimension) shapes. A hardware system with a laser profiler and motion stage was designed to automatically measure 3D shapes. The 3D shape of each member has damage characteristics, such as hole deformation, thread abrasion, excessive clearance, and dents. Damage-detection algorithms for each inspection criterion were developed using machine learning and the geometric features of 3D shapes. The proposed method was validated using temporary equipment samples, with and without damage.

Keywords: automated inspection; damage detection; laser profiling; temporary equipment; temporary structure

1. Introduction

Demands for safety have been steadily increasing in the construction industry, prompting research and practices aimed at preventing safety-related accidents (Cheng *et al.* 2021, Hsu *et al*. 2020, Lee *et al*. 2022, Ghiasi and Malekjafarian 2023, Razavi *et al*. 2024). In particular, temporary structures are a vulnerability factor in terms of construction site safety. Safety-related accidents with severe fatalities in temporary structures account for the largest percentage of accidents at construction sites (Korea Ministry of Employment and Labor 2022). According to the United States Bureau of Labor Statistics, 60 deaths and 4, 500 injuries occur every year owing to accidents in temporary structures (United States Bureau of Labor Statistics 2021). In total, 206 deaths occurred in Korea between 2019 and 2022, due to temporary structures (Korea Ministry of Employment and Labor 2022). Accidents with temporary structures can be caused by various factors such as overloading and poor installation of temporary equipment. Hence, the quality of individual temporary equipment members is a fundamental requirement for accident prevention. Thus, the damage to temporary equipment should be inspected to ensure the quality of each member, as this affects the entire structural performance of the temporary structure. Temporary equipment members are generally reused after quick inspections to ensure quality and prevent accidents.

Quality management of temporary equipment is conducted in each country. As shown in Table 1, because the production and utilization (rental/delivery, site delivery/inspection, installation/operation, and dismantling/removal) of temporary equipment are carried out by the same individual companies in the U.S. and Europe, the quality evaluation standards and systems focus solely on the production phase and related product quality (Underwriters Laboratories Inc. 2023, European Commission 2013). In contrast, Korea and Japan have inspection standards for the quality management of reused temporary equipment (Kim *et al*. 2021). Before and after the delivery of the equipment to the construction site, a visual inspection of the reused temporary equipment is conducted by workers to categorize the grades of each member as A (reuse), B (repair and reuse), or C (disposal), according to the guidelines for quality management. Performance verification tests, such as compression and tensile tests, are conducted by random sampling, if needed. However, the global standards and systems for quality management are insufficient to ensure the quality and performance of temporary equipment. In addition, subjective visual inspection is labor-intensive and unreliable. Thus, the inspection process must be enhanced by developing an automated inspection system based on measurement data.

Measurement-based automatic inspection has been widely employed, particularly in various industrial fields, to ensure product quality. Owing to advances in machine-vision technology, various studies and applications of automated damage inspection using images and 3D shapes

*Corresponding author, Ph.D., Professor,
E-mail: ssim@skku.edu
[a] Ph.D. Student

ISSN: 1738-1584 (Print), 1738-1991 (Online)

Table 1 Global standards for quality management and evaluation of temporary equipment

Cycle of temporary equipment	Korea	Japan	United States	Europe
Production	• Safety certification system[1)] • Korean industrial standards certification[2)]	• Certification system[5)] • Management guidelines for reused temporary equipment [6)]	• UL mark system[7)]	• CE mark system[8)]
Rental	• Safety certification system[1)] • Guidelines on performance standards for reused temporary equipment [3)]			
Delivery to construction site	• Safety certification system[1)] • Quality management system of temporary equipment [4)]			

1) Ministry of Employment and Labor, Korea
2) Korean Agency for Technology and Standards, Korea
3) Korea Occupational Safety and Health Agency, Korea
4) Ministry of Land, Infrastructure and Transport, Korea
5) Ministry of Health, Labor and Welfare, Japan
6) Temporary Construction Industry Association, Japan
7) Underwriters Laboratories Inc, United States
8) Conformite Europeen, Europe

Measurement-based methods generally employ computer vision techniques and 3D shape measurement to detect the deformation and surface damage of an object. A deep-learning-based inspection method was proposed to detect manufacturing defects in the X-ray images of products (Ferguson *et al*. 2018). A deep-learning framework using a single-stage object detection model was developed for manufacturing defect detection in printed circuit boards (Bhattacharya and Cloutier 2022). The manufacturing industry extensively utilizes 3D laser profilers for defect detection and product dimension verification (Keyence Corporation of America 2023). In addition to its application in the manufacturing industry, a few studies have been conducted on civil engineering and maintenance of structures. A robotic sensing system was proposed to detect internal defects in underground water pipes using a 3D laser profiler and stereo vision (Gunatilake *et al*. 2021). An automatic detection system for pavement defects, including cracks and deformations, was developed using 3D pavement data obtained from a laser profiling system (Zhang *et al*. 2018). A 3D laser profiling system was proposed to detect rail surface defects such as abrasion, scratching, and peeling (Xiong *et al*. 2017). Despite such progress, the quality inspection of reused temporary equipment members via computer vision and 3D laser profiling is rarely considered. However, a computer vision-based quality inspection method for reused temporary equipment has been proposed (Kim *et al*. 2022). The inspection system employs deep learning techniques to detect corrosion on the surfaces of temporary equipment. However, it only considers surface corrosion and excludes other damage types related to shape, such as deformation and abrasion, which should also be inspected to ensure the comprehensive quality of the temporary equipment. Thus, a quality inspection system assessing damage related to the shape of reused temporary equipment based on measurement data is required.

This study proposes an inspection method that can automatically identify damage to temporary equipment using 3D shapes. Unlike previous studies that primarily focus on surface-level defects, this research comprehensively analyzes shape-related damages such as dents, thread abrasion, hole deformation, and excessive clearance, which are commonly found in reused temporary equipment according to the inspection standards of Korea. The hardware of the proposed inspection station includes a laser profiler for measuring the 3D shape of the temporary equipment and a motion stage that can move the sensors to scan the entire specimen. A damage-detection algorithm was developed to automatically identify damage using shape measurements, leveraging geometric features to ensure precise detection. The main contributions of this study include the development of a novel hardware system integrating automated 3D shape measurement, implementation of tailored damage-detection algorithms for multiple defect types. These contributions address the limitations of manual inspection methods, enhancing safety, efficiency, and practical applicability in the quality control of reused temporary equipment. The proposed method was experimentally validated using samples of re-used temporary equipment.

2. Background

2.1 Laser profiling

Shape measurement is important in the quality evaluation of reused temporary equipment. Hence, a laser profiler is adopted in this study. A laser profiler is a sensor that can measure the 3D shape of an object (Mathavan *et al*. 2015). The sensor consists of a laser transmitter and camera, as shown in Fig. 1. The laser profiling system employs a triangulation method to calculate the range of information on the surface of an object. A line laser is projected onto the surface of the target object under investigation. The reflected light is captured by the camera and used to generate a range-image, where each pixel represents the distance between the camera and corresponding point on the object (Curless and Levoy 1996). The depth of the target point on the laser line can be calculated using known parameters related to the geometric relationship between the camera and laser transmitter. The parameters include (1) the angle (θ) between the laser

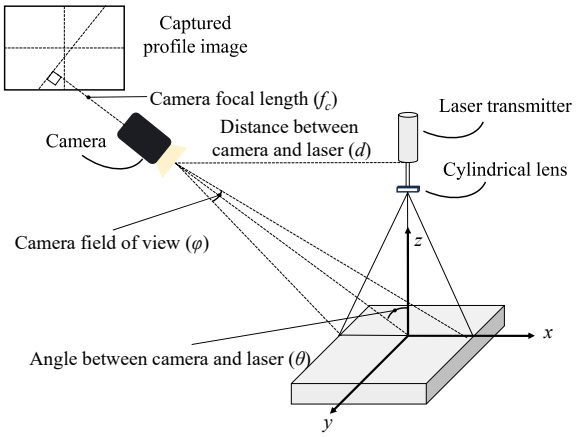

Fig. 1 Principle of laser triangulation

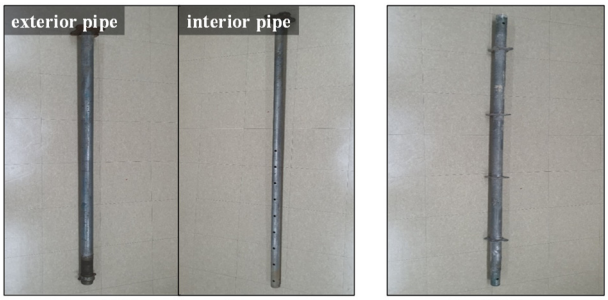

Fig. 2 Targeted type of temporary equipment

projection from a source and optical axis of the camera, (2) baseline distance (d) between the optical center of camera and laser transmitter, (3) camera field of view (φ), and (4) camera focal length (fc). These parameters are determined during the design of the laser profiling system. This process is repeated by moving the laser profile to obtain the depth information of the entire body of the object. Laser profiling systems enable accurate and fast 3D shape measurements compared to other sensor types, such as time-of-flight (ToF)-based LiDAR or stereo vision systems (Lepot *et al*. 2015).

2.2 Targeted types of temporary equipment and damages

The primary function of the temporary equipment is to bolster permanent structures and ensure safe access to workplaces. Among the different types of temporary equipment, false work members and scaffolding play critical roles in temporary structures, as shown in Fig. 2. Falsework members, which are composed of exterior and interior pipes, provide temporary support to partially completed or unstable structures, until they become self-supported. The use of damaged or low-quality falsework members can lead to the collapse of the structures supported by them. A scaffolding structure offers a stable and secure platform for workers at inaccessible or dangerous locations; thus, the use of damaged scaffolding can result in casualties at construction sites. Therefore, the inspection of falsework members and scaffolding is highly emphasized to ensure the safety of temporary structures. This study focuses on two types of temporary equipment.

Inspection of damage related to the shape of the reused temporary equipment is necessary to ensure its quality. This study refers to the inspection standard of reused temporary equipment in Korea, as shown in Table 2, because the standard of Korea is intricately designed to assess quality grades, unlike other countries that lack detailed standards. According to the inspection standards, shape-related damage can be assessed by checking whether the measurement results are outside of specific threshold ranges. Four types of damage, namely hole deformation, thread abrasion, excessive clearance, and dents, are selected in this study (see Fig. 3).

- **Hole deformation**: Holes in the interiors of falsework members are utilized to assemble the exterior and interior parts with support pins, for ensuring support strength. Hole deformation can cause support strength loss, resulting in the collapse

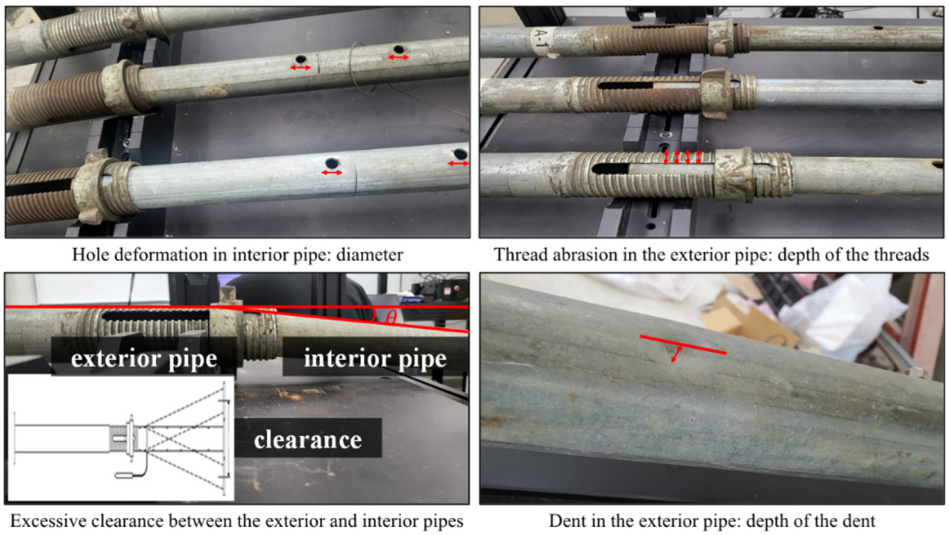

Fig. 3 Targeted type of temporary equipment

Table 2 Example guideline for reused temporary equipment

Type of temporary member	Inspection factor		Assessment criteria
	Item		A, B, C
Falsework member (KS F 8001)	Common	Crack	C: disuse if it exists
		Corrosion	C: disuse if it exists
	Base plate	Deformation	A: no deformation B: deformation exist but can be repaired C: deformation is severe and cannot be repaired
	Interior and exterior pipe	Excessive clearance	A: under 0.72% of total length B: between 0.72% and 0.99% of total length C: above 0.99% of total length (0.72% of V2: 24.5 mm, 0.99% of V2: 33.5 mm)
		Dent	A: no dent B: interior- depth under 4.0 mm; exterior- depth under 6.0 mm C: interior- depth over 4.0 mm; exterior- depth over 6.0 mm
		Hole deformation	A: diameter between 12.8 13.2 mm C: diameter over 13.2 mm and under 12.8 mm
	Support pin	Deformation	B: disuse if it exists
		Missing pin	B: disuse if it exists
		Diameter of pin	A: over 11.5 mm B: under 11.5 mm (substitution)
	Thread	Abrasion	A: depth over 1.4 mm C: depth under 1.4 mm (disuse)
		Defect in assembly part	C: cannot be repaired
Scaffolding (KS F 802)	Flange	Deformation	A: no deformation B: deformation exist but can be repaired C: deformation is severe and cannot be repaired
	General	Dent	A: no dent B: depth under 4.0 mm C: depth over 4.0 mm

of the supported structure. The inspection criterion, "hole deformation" in Table 2 can be determined by examining whether the hole diameter is out of a threshold range.

- **Thread abrasion**: A thread is a part of an exterior falsework member that is used to connect the exterior and interior parts. The thread part allows for height and length adjustments depending on the different locations of the supporting permanent structure. The exterior and interior parts were assembled using a support pin through a hole in the interior part, fixed to the threaded part. Inspection of thread abrasion is necessary because the supporting capacity of a falsework member can be lost if the thread is abraded. Thread abrasion was determined by measuring the depth of each thread line according to the inspection criteria.
- **Excessive clearance**: The clearance between the exterior and interior pipes of a falsework member can significantly affect the overall structural integrity of the falsework. Proper clearance ensures that the loads are evenly distributed and undue stress on any part of the falsework is avoided. The length of the falsework member can be extended by changing the location of the pinhole in the interior pipe. Clearance is defined as the vertical displacement of the interior pipe when the length of the falsework member is at its maximum.
- **Dent**: A dent is a visible deformation or indentation on the surface of temporary equipment. Dents can occur because of impact, overloading, or accidents during use. Severe stress can lead to stress concentration in temporary equipment, potentially initiating cracks or failures that can compromise the structural integrity and functionality of the entire temporary structure. The inspection criterion, "dent" in Table 2 can be determined by examining whether the depth of a dent exceeds a threshold.

3. Proposed inspection method for temporary equipment

This paper proposes an automated system tailored for the quality control of temporary equipment using a measured 3D shape. The inspection system comprises of two main components: (1) 3D shape measurement using an inspection station with a laser profiler and motion stage and (2) damage detection algorithms for each damage type (i.e., dent, thread abrasion, hole deformation, and excessive clearance). The 3D shapes of multiple pieces of temporary equipment were measured using a laser profiler moving

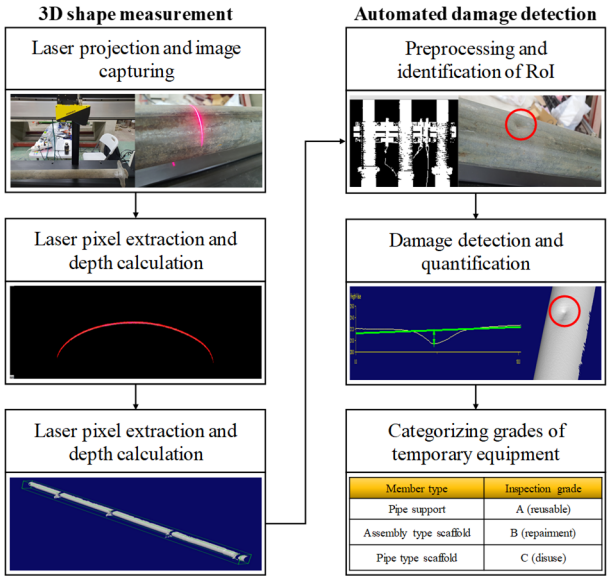

Fig. 4 Overview of the automated inspection system

along a motion stage. The laser profiler projects a laser onto the specimen, and the projected laser is captured by a camera. Subsequently, the laser pixel in the captured image is extracted, and a depth calculation is conducted using the laser triangulation method. The final 3D shape is registered using the scale information from an encoder in the motion stage. Damage detection was performed on the inspection items according to the type of temporary equipment, utilizing the measured 3D shapes. The final grade, utilized for the quality control of temporary equipment, was derived from the result of damage detection. The mechanism of the automated inspection system is illustrated in Fig. 4. This section describes the proposed inspection system in terms of the hardware system and damage detection algorithms.

3.1 Hardware system and 3D shape measurement

The hardware system of the proposed method was designed to acquire the 3D shape of temporary equipment for damage detection. As shown in Fig. 5, the hardware system of the inspection station has a laser profiler for data acquisition and motion stage for moving the sensors. The inspection station has a flat space for the placement of temporary equipment, above which the motion stage is installed. The laser profiler attached to the motion stage can travel from one end to another to scan the entire body of the inspected temporary equipment. The motion stage is equipped with an encoder that provides the current location of the sensors and distance based on the orientation. The laser profiler acquired the 3D shape of the temporary equipment using laser triangulation, as described previously. The laser profiler was installed at a specific distance away from the flat space such that the measurement range simultaneously covered the three temporary pieces of equipment. The laser profiler and motion stage were connected to a computer that controlled the inspection system, stored data, and conducted damage detection.

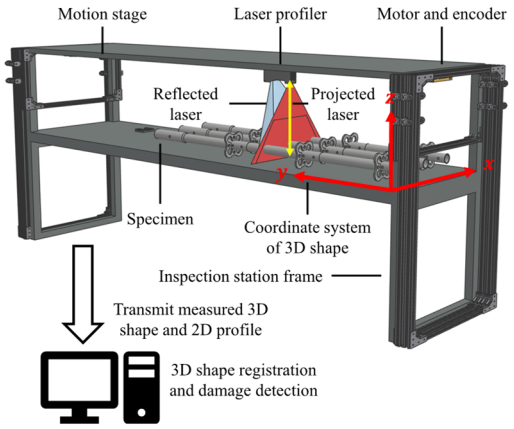

Fig. 5 Hardware system: inspection station

The configurations of 3D shape measurements need to be determined by considering the different dimensions and material properties of each type of temporary equipment. The sensitivity of the laser detection and exposure time were set by considering different material properties and conditions, such as the reflectance of the surface of temporary equipment. Most re-used temporary equipment has dark and low-reflectance surfaces compared to newly manufactured components due to contaminants from repeated use. The exposure time and gain values were set higher to improve a quality of range image and 3D shape.

- **Exposure Time:** Longer exposure improves detection on dark surfaces but risks saturation on highly reflective materials.
- **Gain Value:** Higher gain amplifies weak signals but increases noise, reducing accuracy.
- **Dynamic Range:** A wider range allows detection of diverse materials but may reduce resolution for specific features.

Because the dimensions of each type of temporary equipment are known, a region of interest (ROI) in the captured image of the projected laser can be determined to enhance the computational efficiency and increase the measurement frequency, enabling a high-resolution range-image. The resolution of the range-image, which is important for precise damage detection, can be determined by various parameters such as step-per-line and distance-per-cycle, related to encoder pulses. In the laser-profiling system shown in Fig. 1, the line laser is projected parallel to *x*-axis, and the laser profiler moves along the *y*-axis, which is parallel to the motion stage. The resolution of the captured profile image on the *x*-axis is fixed when the size of the image sensor in the laser profiler and measurement ranges are determined. The resolution in the *y*-axis is the product of the step per line (pulses/pixels) and the distance per cycle (mm/pulses). When the laser profiler moves along the motion stage, the encoder connected to the motor transmits electronic pulses representing the physical distance of the sensor. Step-per-line refers to the number of encoder pulses required to acquire a single projected laser line. If the step-per-line is small, the laser profile acquires more data points along the *y*-axis, leading to a higher

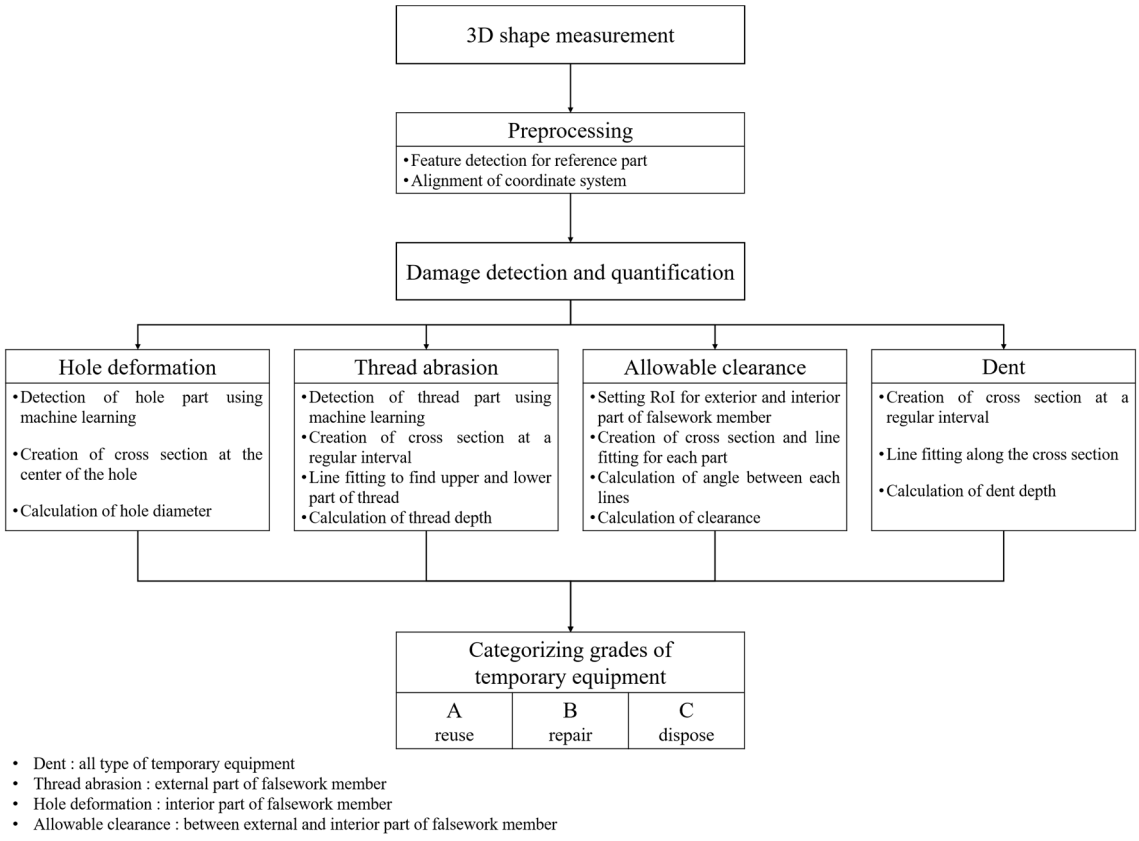

Fig. 6 Flowchart of damage detection algorithms

resolution. Distance-per-cycle indicates the spacing between encoder pulses. If distance per cycle is 0.01 mm/cycle, and the laser profiler moves 40 mm away, the distance is converted into 4,000 pulses of electronic signal. These parameters should be appropriately configured based on the required inspection accuracy, speed, and hardware performance, including those of the motor and encoder. In this research, the resolution of the profile in the *y*-axis was set as a maximum of 0.1 mm/pixel, and this was sufficient for precise damage detection. The inspection speed and scan range were determined by considering the dimensions and shape of each type of temporary equipment.

3.2 Damage detection of temporary equipment

Damage detection algorithms tailored to each type of damage selected in this study were developed to assess the quality of temporary equipment according to the criteria described in Table 2. A flowchart of the damage detection method is shown in Fig. 6. After completing the shape measurement process described in Section 3.1, the measured 3D shape data, including the projection of the entire registered range-image onto the *xy*-plane and arrangement of the coordinate system, was pre-processed. Damage detection and quantification were performed for each damage type, including dents, hole deformation, excessive clearance, and thread abrasion, by utilizing the geometric features of the 3D shape and projected range-image. Finally, the grade of the temporary equipment, used for further quality management, was determined. The specifications of the damage detection and quantification algorithms for each damage type are presented in this section.

In the pre-processing stage, the coordinate system in the measured 3D shape was transformed for automated damage detection, as shown in Fig. 7. Let W_i denote the coordinate system of the original projected range-image for the i^{th} measurement. Note that W_i varies in inspection each scan because each temporary piece of equipment is loaded in slightly different positions, and the measurements are affected by the electrical noise in the laser profiler. Because a ROI is desired for automation in damage detection, each coordinate system of the measured range-images should be transformed into a consistent coordinate system with respect to the individual temporary equipment. To transform W_i, we select a fixed area that has distinctive features and can be used to define a consistent coordinate system (W_{fixed}). For example, a region with a clamp that holds temporary equipment can be used as a fixed area. The patterns of the fixed area are trained using a machine-learning algorithm for automatic detection of the region. Within this area, the pattern that is the most similar to the trained pattern geometry is detected. Finally, the transformation from W_i to W_{fixed} is computed, which is a rigid-body transformation that enables rotation and translation without any alterations in shape or size. During each inspection, each measured range-image is transformed into a reference coordinate system. The automated damage detection and quantification algorithms for each damage type are as follows.

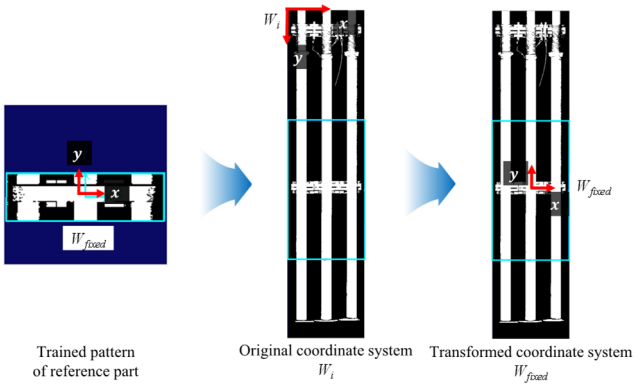

Fig. 7 Transformation to the fixed coordinate system

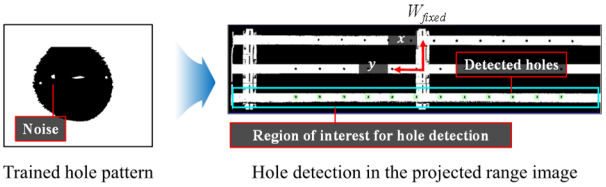

Fig. 8 Hole detection in the projected range-image

Hole deformation

The damage detection algorithm for hole deformation includes hole localization and diameter estimation. Automated hole detection using machine learning is necessary because the locations of the holes are unknown. The hole pattern shown in Fig. 8 was designated for training. The model trained with the hole pattern was applied to detect holes within the ROI for each piece of equipment at the inspection station. Once a hole pattern is identified, its diameter must be determined. As the projected range-image can contain noise, as shown in Fig. 8, utilizing the original range-image with depth information is more appropriate for reliable estimation of the hole diameter. In the region of the detected hole pattern, multiple cross-sections, which are parallel to z-axis and either x- or y-axis, are generated. For each group of cross sections in the x- and y-axes, edge points are extracted to compute the hole diameter (see Fig. 9). In each group, the maximum distance between the edge points is used to estimate the hold diameter. Subsequently, the inspection criteria with the hole diameters in both x- and y-directions are considered to determine the grade (Grade A: diameter between 12.8 and 13.2 mm; Grade C: diameter over 13.2 mm or under 12.8 mm).

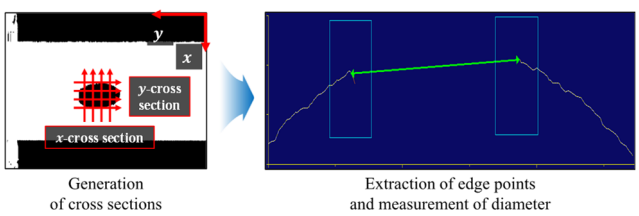

Fig. 9 Measurement of hole deformation

Thread abrasion

The thread abrasion detection process is divided into two parts: (1) detection of thread and (2) measurement of thread depth. Similar to the detection algorithm for hole deformation, a region of the thread in the projected range-image is designated for pattern training. After detecting the thread pattern using the trained model, multiple cross sections are created in the original range-image at regular intervals (e.g., 1–2 mm), as shown in Fig. 10. In each cross-section, the lowest points in the threads at both ends are extracted to obtain a baseline (Fig. 10). The depth of each thread is the distance between the baseline and highest point of the thread as described in Fig. 11. The obtained thread depth is used to determine the grade according to Table 2 (Grade A: depth > 1.4 mm; Grade C: depth < 1.4 mm).

Excessive clearance

The inspection process for excessive clearance involves (1) line fitting of the exterior and interior pipes and (2) computation of the clearance. First, a ROI is designated in the exterior and interior pipes, excluding the thread part, determined in the previous stage (i.e., thread abrasion inspection). To measure the maximum angle between these two parts, a cross-section at the middle of the specimen is generated parallel to the yz-plane. Within the cross section, the equation of the line of the exterior and interior pipes is computed by line fitting along the ROIs using linear regression, as shown in Fig. 12. Let the maximum angle be θ, and the direction vector of the exterior and interior pipes be $\boldsymbol{d_e}$ and $\boldsymbol{d_i}$, respectively. The maximum angle and associated clearance can be computed as follows

$$C = 2L\cos\theta = 2L\frac{d_e \cdot d_i}{|d_e| \cdot |d_i|}$$

where C is the clearance and L is the length of the interior pipe. As the total length of the interior pipe is known from the measured 3D shape, the clearance at the maximum angle can be computed using Eq. (1). The calculated

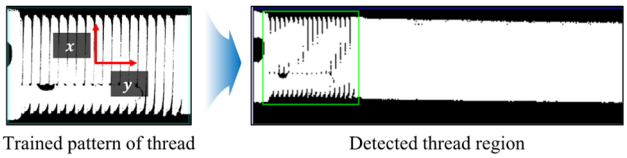

Fig. 10 Thread pattern training and detection in the projected range-image

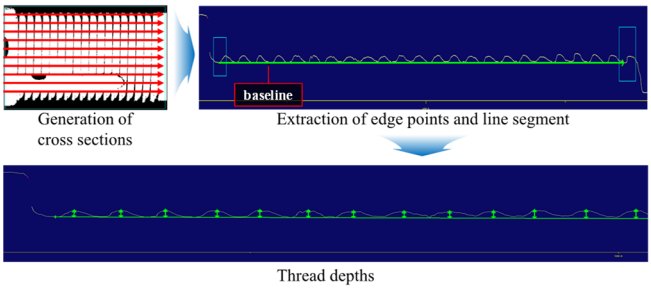

Fig. 11 Detection of thread abrasion

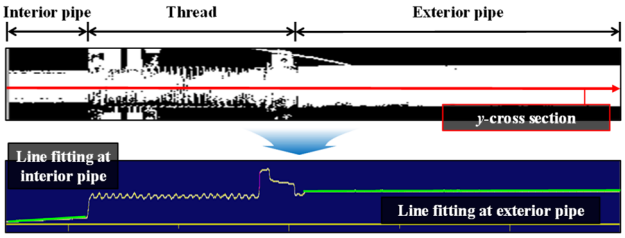

Fig. 12 Calculation of excessive clearance between the exterior and interior pipes of a falsework member

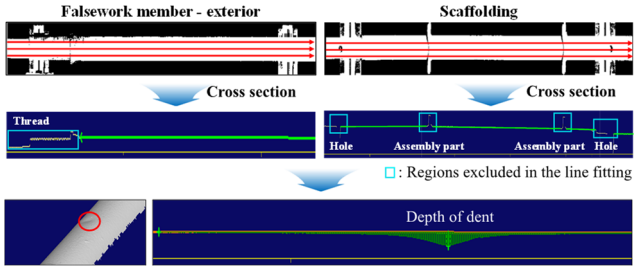

Fig. 13 Calculation of dent depthshpg

clearance is categorized into three grades according to the inspection criteria (Grade A: under 0.72% of total length; Grade B: between 0.72 and 0.99% of total length; Grade C: above 0.99% of total length).

Dent

Dents in false work members and scaffolding can be detected by inspecting abnormal depth values in the range-image. Because a dent can occur at any location on temporary equipment, the entire area of the specimen should be inspected. As shown in Fig. 13, multiple cross-sections parallel to the *yz*-plane were generated at regular intervals. Regions of the thread, hole, and assembly parts that were not of interest were excluded. The protruding

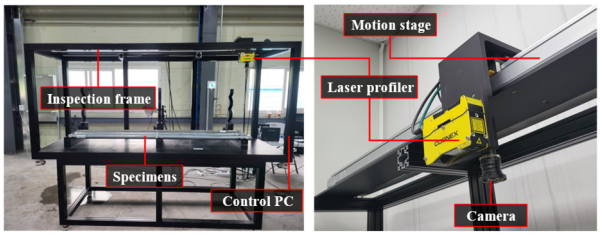

Fig. 14 Experimental setup

assembly parts can be found using higher z-coordinate values. To detect dents and calculate their depths in the remaining regions, line fitting was conducted using linear regression for each cross-section. The depths can be computed by measuring the distances from each point on the cross-section to the fitted line. If the maximum value of the computed depth is greater than the prescribed threshold, the corresponding point is considered a dent. The detected dent was then categorized into one of three grades according to the inspection criteria (Grade A: no dent; Grade B: dent depth < 4.0 mm for interior false work member and scaffolding, depth < 6.0 mm for exterior false work member; Grade C: otherwise).

4. Experimental validation

4.1 Experimental setup

Experimental validation of the proposed automated inspection strategy was conducted using samples of reused temporary equipment. The hardware system described in Section 3.1 was manufactured as shown in Fig. 14, considering the automation of inspection. The specifications of the inspection system are listed in Table 3. The dimensions of the inspection station were 2,560 mm × 800 mm × 2,000 mm, and a maximum of three temporary

Table 3 Hardware specification

Component	Function	Specification
Laser profiler	3D shape measurement by laser triangulation	• Model: Cognex 3DL-4300 • Measurement range - x-axis: 95–460 mm - z-axis: 180–745 mm • Resolution - x-axis: 49.6–239.6 μm - z-axis: 6.9–147.5 μm • Scan rate: 4 kHz
Motor and linear stage	Enabling laser profiler to move in the inspection range	• Mechanical type: Linear motion guide • Guide mechanism: Ball screw • Motor type: Servo motor • Maximum speed: 1250 mm/s • Sensors: Two limit sensors and one home sensor
Encoder	Registering 3D shape in real scale unit along the y-axis	• Type: 22-bit • Resolution: 4194304 pulses/rev
Inspection station frame	Loading maximum three temporary equipment to be inspected	• Length: 2,560 mm • Width: 800 mm • Height: 2,000 mm

Table 4 Types and number of samples

Types of damage		Number of samples (Falsework member: 30, Scaffolding: 30)		
		Grade A	Grade B	Grade C
Hole deformation (Falsework member)		24		6
Thread abrasion (Falsework member)		22		8
Excessive clearance (Falsework member)		13	9	8
Dent	Falsework member	25	3	2
	Scaffolding	23	4	3

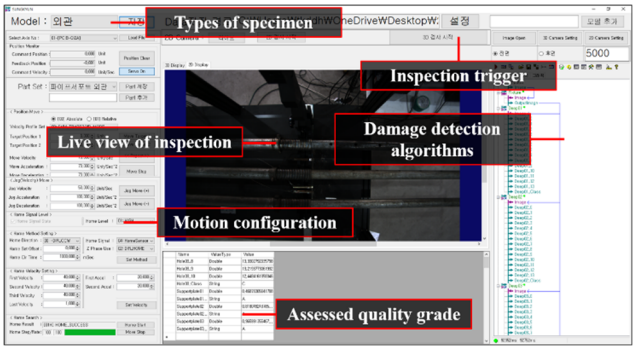

Fig. 15 Automated inspection software

equipment members could be loaded. A laser profiler (Cognex 3DL-4100) was used to acquire the 3D shape of the temporary equipment. The laser profiler was installed at a height of 800 mm from the surface of the inspection station within the maximum working distance such that the measurement range simultaneously covered three pieces of temporary equipment. A 2D camera was used to verify the inspection process. A control computer was installed to operate the inspection system. Considering the distribution of the quality grades of the specimens utilized in the experiment (Table 4), 30 scaffoldings and 30 falsework members were prepared.

In addition, an automated inspection software for temporary equipment was developed to validate the practicality and applicability of the proposed method. The functions of the automated inspection software include the control of the motion stage and data acquisition, as shown in Fig. 15. When a type of target temporary equipment is selected, the corresponding configurations, including damage-detection algorithms and motion parameters such as velocity and scan length, are loaded automatically. These configurations can be modified in real time using the automated inspection software. A live view from the camera installed next to the laser profiler enabled us to determine whether the inspection process was performed appropriately. The automated inspection software enhanced the efficiency and reliability of the inspection processes.

When three specimens were loaded on the inspection station, the 3D shape measurement was performed twice (front and back of specimens) because the laser profiler could cover only 50% of the surface of the object. Possible damage to each type of temporary equipment can be inspected simultaneously. The results of the quality inspection using the proposed method were compared with those of manual inspection using calipers and laser distance meters. The experimental results are presented in the subsequent section.

4.2 Experimental results

The results of quality inspection using the automated inspection system and a comparison with the results from the precise inspection are presented in Table 5. The number of accordant quality grades and accuracy for each damage type were calculated. The average difference was 8.0%, and the proposed method showed good agreement with the manual inspection. In particular, the thread abrasion showed the lowest difference of 3.4%, proving the capability of the proposed method for damage detection in complicated shapes. The maximum difference was observed in the inspection of excessive clearance in falsework members because the length of the interior pipe that should be extended to the maximum depended on the inspectors, leading to differences in the maximum angle. The proposed automated inspection system offers reliable quality inspection of temporary equipment, along with advantages in the productivity and efficiency of the inspection process.

Table 5 Comparison between the proposed method and manual inspection

Types of damage		Inspection result (Number of specimens with accordant quality grade / total number)			
		Grade A	Grade B	Grade C	Difference (%)
Hole deformation	Falsework member	22 / 24		6 / 6	6.7
Thread abrasion	Falsework member	22 / 22		7 / 8	3.4
Excessive clearance	Falsework member	12 / 13	8 / 9	6 / 8	13.4
Dent	Falsework member	22 / 25	3 / 3	2 / 2	10.0
	Scaffolding	22 / 23	4 / 4	2 / 3	6.7
Difference (%)		**8.0**			

5. Conclusions

The quality of the reused temporary equipment is essential to ensure the structural integrity of the temporary structure and safety of workers. Subjective manual inspection, which is a common practice in the quality management of temporary equipment, is inefficient and unreliable. Although recent machine-vision studies have demonstrated a wide variety of real-world applications for automated damage detection, these approaches have not been fully considered for the management of temporary equipment. This paper proposed an automated inspection method for temporary equipment based on measurement data to identify shape-related damage.

The proposed method can automatically inspect multiple types of damage that occur in reused temporary equipment. Four types of damage, namely hole deformation, thread abrasion, excessive clearance, and dents, were considered in damage detection. The developed inspection station includes a laser profiler, motion station, and control PC. The 3D shape can be measured using a laser profiler that moves on the motion stage such that the entire body of the specimen is scanned. Damage-detection algorithms were developed for each damage type by utilizing the geometric features of the measured 3D shape. Both the hardware system and damage-detection algorithms were designed while considering the automation process of the inspection.

This automated inspection method was experimentally validated using samples of reused temporary equipment. The quality grades of 30 scaffoldings and 30 falsework members were assessed using the proposed method, and the results were compared with those of manual inspection. The results showed an average difference of 8.0%, proving that the proposed inspection method can detect damage of temporary equipment accurately and reliably. Thus, the proposed method can contribute to reducing the reuse of low-quality temporary equipment at construction sites.

Future work will aim to expand the system's inspection capabilities by integrating multi-modal data collection, combining 3D shape data with 2D imaging, and incorporating additional damage types, such as surface corrosion, dimensional variations, and deformations in critical components like pipe diameters and flanges of external pipe supports. These advancements will further enhance the robustness of the system, ensuring more comprehensive quality control and contributing to safer construction practices.

Acknowledgments

This work was supported by a Korea Agency for Infrastructure Technology Advancement (KAIA) grant, funded by the Ministry of Land, Infrastructure, and Transport (Grant RS-2020-KA156488).

References

Cheng, K., Shan, J. and Liu, Y. (2021), "Feature-based image stitching for panorama construction and visual inspection of structures", *Smart Struct. Syst., Int. J.*, **28**(5), 661-673. https://doi.org/10.12989/sss.2021.28.5.661

Bhattacharya, A. and Cloutier, S.G. (2022), "End-to-end deep learning framework for printed circuit board manufacturing defect classification", *Sci. Rep.*, **12**(12559). https://doi.org/10.1038/s41598-022-16302-3

Curless, B. and Levoy, M. (1996), "A volumetric method for building complex models from range images", *Proceedings of the 23rd Annual Conference on Computer Graphics and Interactive Techniques*, New Orleans, LA, USA, August.

European Commission (2013), CE marking of construction products step by step. https://ec.europa.eu/docsroom/documents/12308/attachments/1/translations/en/renditions/native

Ferguson, M.K., Ronay, A., Lee, Y.T. and Law, K.H. (2018), "Detection and segmentation of manufacturing defects with convolutional neural networks and transfer learning", *Smart Sustain. Manuf. Syst.*, **2**. https://doi.org/10.1520/SSMS20180033

Ghiasi, R. and Malekjafarian, A. (2023), "Feature subset selection in structural health monitoring data using an advanced binary slime mould algorithm", *J. Struct. Integr. Maint.*, **8**(4), 209-225. https://doi.org/10.1080/24705314.2023.2230398

Gunatilake, A., Piyathilaka, L., Tran, A., Vishwanathan, V.K., Thiyagarajan, K. and Kodagoda, S. (2021), "Stereo vision combined with laser profiling for mapping of pipeline internal defects", *IEEE Sens. J.*, **21**(10), 11926-11934. https://doi.org/10.1109/JSEN.2020.3040396

Hsu, T.Y., Pham, Q.V., Chao, W.C. and Yang, Y.S. (2020), "Post-earthquake building safety evaluation using consumer-grade surveillance cameras", *Smart Struct. Syst., Int. J.*, **25**(5), 531-541. https://doi.org/10.12989/sss.2020.25.5.531

Keyence Corporation of America (2023), Applications of laser profiling system to industries. https://www.keyence.com/solutions/applications/

Kim, H., Lim, J., Won, J.-H., Kwon, J.-H. and Kim, S. (2021), "Suggestion of safety certification standards and performance evaluation methods for fabricated mobile scaffold in South Korea", *Int. J. Environ. Res. Public Health*, **19**(1), 133. https://doi.org/10.3390/ijerph19010133

Kim, A., Lee, K., Lee, S., Song, J., Chung, S. and Kwon, S. (2022), "Synthetic data and computer-vision-based automated quality inspection system for reused scaffolding", *Appl. Sci.*, **12**(19), 10097. https://doi.org/10.3390/app121910097

Korea Ministry of Employment and Labor (2022), Industrial accident status. https://www.moel.go.kr/policy/policydata/view.do?bbs_seq=20230300058

Lee, S., Gil, S.-K., Cho, S., Shin, S.W. and Sim, S.-H. (2022), "Wireless safety monitoring of a water pipeline construction site using LoRa communication", *Smart Struct. Syst., Int. J.*, **30**(5), 433-446. https://doi.org/10.12989/sss.2022.30.5.433

Lepot, M., Stanic, N., Clemens, F.H.L.R., Catieau, M., Goes, B.H.G. (2015), "Laser profiling: A promising technique to accurately assess pipe state and roughness", *Proceedings of the 10th International Urban Drainage Modeling Conference*, Mont-Sainte-Anne, Quebec, Canada, September.

Mathavan, S., Kamal, K. and Rahman, M. (2015), "A Review of three-dimensional imaging technologies for pavement distress detection and measurements", *IEEE Trans. Intell. Transp. Syst.*, **16**(5), 2353-2362. https://doi.org/10.1109/TITS.2015.2428655

Razavi, M., Hadidi, A. and Ashrafzadeh, F. (2024), "Feature extraction based on dynamic response measurements for structural damage identification: a comparative study", *J. Struct. Integr. Maint.*, **9**(2), P. 2364125. https://doi.org/10.1080/24705314.2024.2364125

Underwriters Laboratories Inc. (2023), Marking and labeling

systems program. https://www.ul.com/services/marking-and-labeling-systems-program

United States Bureau of Labor Statistics (2021), Occupational Safety and Health Administration. https://www.osha.gov/scaffolding

Xiong, Z., Li, Q., Mao, Q. and Zou, Q. (2017), "A 3D laser profiling system for rail surface defect detection", *Sensors*, **17**(8), 1791. https://doi.org/10.3390/s17081791

Zhang, D., Zou, Q., Lin, H., Xu, X., He, L., Gui, R. and Li, Q. (2018), "Automatic pavement defect detection using 3D laser profiling technology", *Autom. Constr.*, **96**, 350-365. https://doi.org/10.1016/j.autcon.2018.09.019